33rd Symposium on Naval Hydrodynamics
Osaka, Japan, 31 May-5 June 2020

Hydrodynamic Design of Propulsion Devices taking into account Full Scale Roughness Effects

Keunjae Kim[1], Michael Leer-Andersen[1] and Sofia Werner [1]
([1]SSPA Sweden AB, Sweden)

ABSTRACT

This paper addresses the effects of hull roughness on propulsion performance of ships and demonstrates the importance of taking full scale roughness effects into account when designing propulsion devices. The investigation of the hull roughness effect was performed numerically using SHIPFLOW with the built in roughness model based on the assumption that hull surface roughness is uniformly distributed and can be characterized by the equivalent sand roughness.

The ship investigated is a SSPA VLCC with three typical energy saving devices (ESDs), which include a duct, a standard pre-swirl stator (PSS) and two SSPA generic ESDs (GKD_M and GKD_F). As an initial validation study, numerical simulation and model tests were carried out for the bare hull with two surface conditions: smooth and rough surface. The results from numerical simulation were validated against towing tank tests and clearly indicates a gradual change of flow characteristics/propulsion performances with hull roughness growth: thickening of boundary layer, increase of resistance and propulsion properties (T, Q and RPM). Following the model scale study, full scale simulations have been performed. The results from full scale simulations confirm the trend in increase of EHP and DHP as roughness grows, but even much faster in full scale compared to model scale.

This paper will further focus on combined hull roughness and scale effects in the design of propeller/ESD and prediction of the performance of a ship. A quite interesting finding is that the roughness is not always affecting in negative direction. The propeller can be operating in more favorable conditions with higher angle of attack due to the thickening of the boundary layer with the increase of hull roughness. This can directly lead to the improvement of propulsive efficiency and in turn result in further power reduction with the use of ESDs.

This paper will discuss additional steps needed to take into account of hull roughness in design optimization process of propeller and ESDs and present design methodology for the successful development of propellers and ESDs performing well in actual operational conditions.

INTRODUCTION

The hydrodynamic design of propeller is not a simple task as they operate in the complex wake field around the stern of the ship and further increase the complexities even more when ESDs are installed. In addition, it is not an easy task to predict reliably the energy saving potential of ESD. This is because several effects are involved and the problem is very complex. Therefore, a traditional design and prediction method does not necessarily provide correct solutions or conclusions.

Among many other complexities involved in the design of propulsion devices, the two most important effects, scaling and roughness effect will be addressed in this paper. Scaling is a known problem when designing and testing propellers and ESDs, as they operate around the stern of the ship where the scale effects of model test are most pronounced. SSPA, and also other institutions within the community, has recognized that there can be risk if propeller/ESDs are developed and applied in a standard routine process only based on model scale, not taking into the full scale flow effect. SSPA has performed a series of extensive research studies quantifying the scale effects on the inflow to the propeller/ESDs. The first work performed was an extensive SHIPFLOW self-propulsion simulation made for several ship types (Kim et al 2011) and for ESDs (Kim et al 2012 and 2012). These simulation studies revealed that many propellers are in possible risk of poor performance in full scale as they are operating with negative angle of attack. A main reason for this is that the performance prediction and propeller design methods are still based on empirically scaled full scale wake from the model scale wake measured in model tests. The problem is that the scaling procedure is relatively simple and certainly not very robust to capture fully the scaling effects on the transverse flow components or even on vortex structures like bilge vortices. This finding has led to a close review of the reliability of current performance prediction and propeller design practice. An important recommendation made from two case studies is the use of full scale wake predicted by CFD. CFD can solve this problem offering the capability of evaluating the detailed flow characteristics in both model and ship scale from CFD simulations. The first study (Kim 2011) has shown that full understanding of propeller-hull wake interaction from full scale CFD self-

propulsion simulation is important in avoiding misinterpretation and over-optimistic prediction of propulsion efficiency. The second propeller design study (Kim 2012) demonstrated possible improvement potential of propulsion efficiency by 1 ~ 2 percent if the propeller pitch and camber loading are optimized with respect to mean propeller angle of attack from full scale self-propulsion simulation instead of wakes scaled empirically or simulated from full scale resistance simulation.

The scale effects of energy saving of typical ESDs have also been investigated and the results were presented at previous ONR symposiums. A design optimization study of pre-swirl stator (PSS) for an Aframax product carrier has been performed by full scale self-propulsion simulation, confirmed by model tests to validate through sea trial (Kim 2012). Encouraged by the first successful design application of PSS, four different ESDs were investigated by full scale CFD simulations to analyze the scale effects on the energy saving mechanisms of the devices for a VLCC (Kim 2014). CFD can provide detailed insights into the resulting flow around the propeller/ESDs, which can be used for evaluating the potential for propulsion efficiency improvements. An important finding obtained is that the energy savings predicted by CFD for ESD is Reynolds number dependent: the ESDs investigated are quite effective in reducing the power in model scale, but less effective in full scale. Another finding is that the scale effects are varying dependent on type of ESD; a duct is not actually working as an energy saver in full scale while a PSS is less sensitive to scale effects than SSPA generic ESDs, OKD and GKD (combination of duct and PSS). Savings predicted by CFD in full scale is only a half for OKD and a third for GKD as compared with those obtained in model scale. A similar result has been reported by Visonneau et al (2016). They have performed a model and full scale self-propulsion simulation using ISIS-CFD for Japan Bulk Carrier (JBC) with a duct as an ESD, and compared the gain of propulsive efficiency predicted by CFD and model tests. Their study fully confirms that the duct can not be regarded as an energy saver; 6.5% improvement in propulsion efficiency predicted by model tests from NMRI while no practical improvements were estimated by CFD. This feature is important in avoiding misinterpretation and over-optimistic predictions by model tests with extrapolations to full scale. This should be highlighted in public domain to raise awareness of the importance of full scale CFD simulation coupled to model testing to make sure that the optimum propeller/ESD design obtained from model tests could still be the optimum in full scale operation.

Another problem addressed in the present paper is hull roughness effect. Hull surface condition plays an important role for ship performances for new-built ships as well as ships in operation as the drag penalties are often substantial due to hull roughness. Accordingly, there has been numerous investigations on roughness effects in the past, but limited to theoretical study focused on frictional resistance or experimental study on flat plate in lab scale. To the best of the authors' knowledge, there are not many practical studies how the roughness should be taken into account in the process of performance prediction, ship design and operational practices found in open literature.

It is well known that the increase of resistance for newly build condition is simply added by the roughness allowance based on empirical formula in ITTC78 performance prediction method. However, the hull roughness effect has been rarely discussed in the ship design phase. An early paper on this issue was presented by Guird (2013) who claimed that the full scale wakes predicted for a 180m mid-size tanker with rough hull surface is much closer to the corresponding model scale wake for smooth surface and thus the power saving observed at full scale is about the same as at model scale. This is certainly a good news for our community, especially ESD manufacturers, but there is quite different results presented by Eca (2010) at the 28th Symposium, showing some degree of increase of boundary layer thickness but more closer to the corresponding full scale wake for smooth surface with the growth of sand grain roughness height k_s up to 300 μm.

This paper will address the two most important scale and roughness effects on the change of flow characteristics, which directly resulted in the increase of EHP/DHP and all propulsive factor (thrust, torque and RPM). The same ship and three ESDs investigated in the previous projects are reused as test cases. Numerical simulations have been performed to investigate the effects of roughness on the change of flow characteristics and performances of a ship not only in model scale but also in full scale. Roughness simulations were performed at the design speed and full load condition with the sand grain roughness height k_s ranging from 0 to 500 μm. As for validation study, model tests were carried out for the bare hull with two surface conditions for the ship model: smooth and rough surface.

This paper describes how hull roughness should be taken into account in the design optimization process of propeller and ESDs and in the interpretation of the efficiency gain based on better understanding of physical energy saving mechanisms of ESDs to provide a confidence in the proposed ESDs as a real energy saver.

TEST HULL

The test ship is a standard VLCC representing the state of the art in design today. For proprietary reasons the exact lines cannot be shown, but a perspective view of hull is given in **Figure 1**. The main dimensions are: length between perpendiculars (L_{PP}) 320m, beam (B) 60.0m and draft (T) 21.0m. The propeller tested is a fixed, right turning, four bladed propeller.

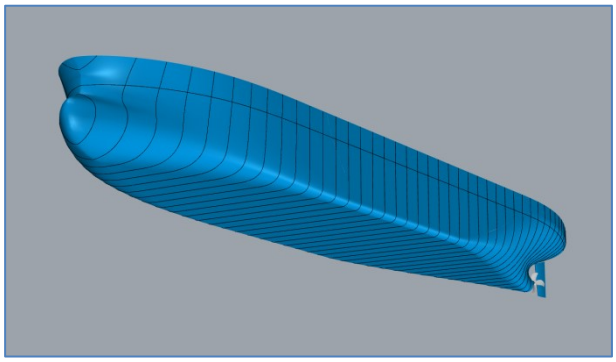

Figure 1: Perspective view of hull geometry.

ESDs INVSTIGATED

In the paper, three different types of ESDs have been investigated; they include a wake equalizing duct (WED), a standard pre-swirl stator (PSS) and SSPA generic ESDs; GKD (duct with inner/outer side stator blades). The WED consist of two half-ring or full ducts of foil section installed on the stern ahead of the propeller (see **Figure 2**). It is claimed that the overall propulsive efficiency can be improved by reduction of hull resistance by reducing the amount of separation over the afterbody of the ship and net thrust generated by the duct.

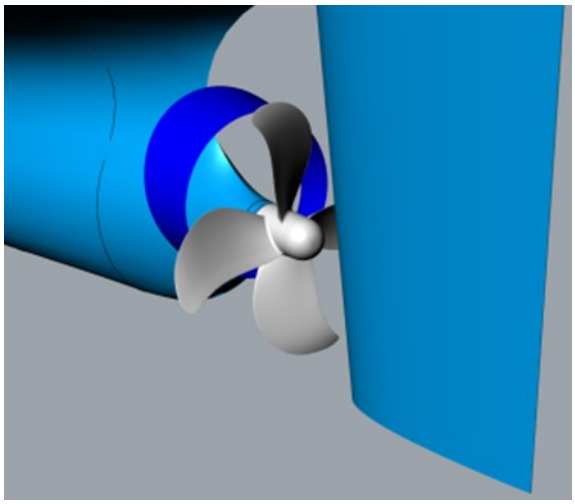

Figure 2: Wake equalizing duct

The PSS is a device mounted on the stern boss just upstream of the propeller (see **Figure 3**). It is designed to generate pre-swirl flow to the propeller in order to gain a favorable interaction with the propeller that improves the propulsive efficiency and results in a power reduction.

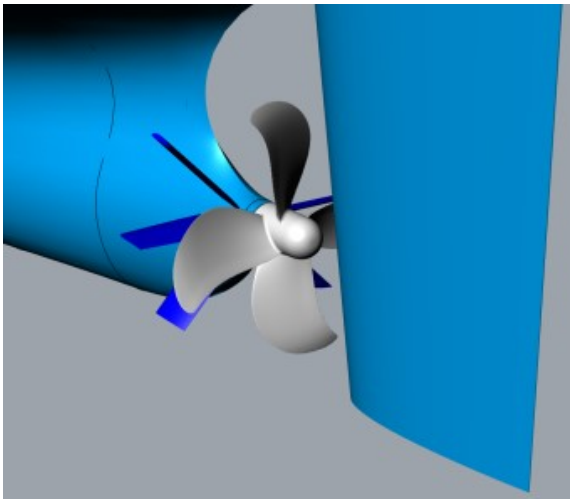

Figure 3: Pre-swirl stator

SSPA own generic ESD, GK duct is developed based on the energy saving mechanisms discussed above, but focusing more on pre-swirl generated on port upper side instead of starboard lower side. As can be seen in **Figure 4**-Figure **5**, the GK duct is composed of a combination of duct and stator blades and the base GK duct configuration has three port outside stator blades mounted on duct and two inside stator blades connected between the duct and hull. The diameter of the duct is about the same as the radius of the propeller and so the duct is positioned within relatively thin viscous boundary layer wake from the ship hull. Two GK ducts were investigated; the initial duct is designed for model scale performance (denoted as GKD_M, see **Figure 4**) and GKD_F which is optimized for full scale performance by adjusting the size and position of the duct and stator blades (see **Figure 5**).

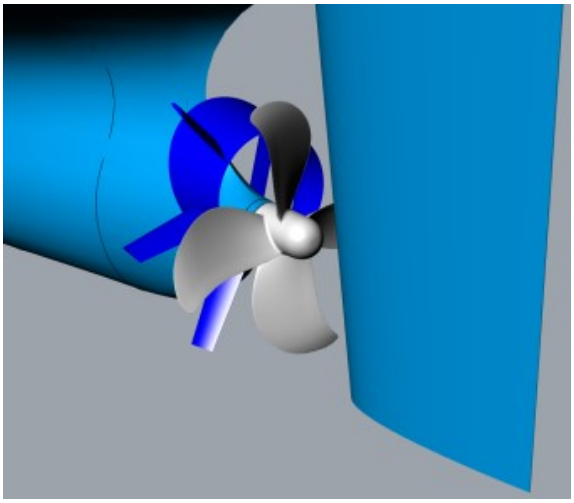

Figure 4: SSPA generic ESD optimized for model scale, GKD_M

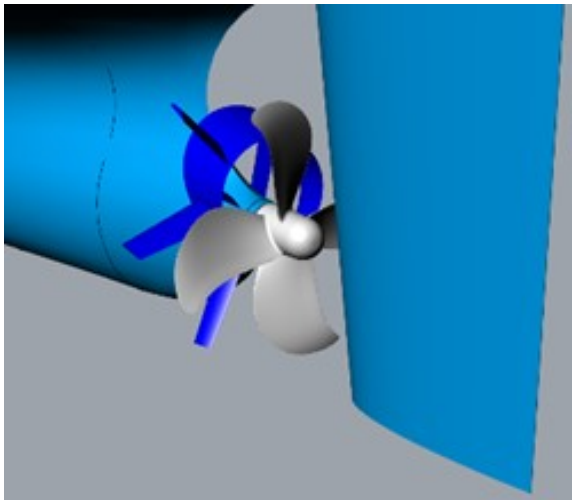

Figure 5: SSPA generic ESD optimized for full scale, GKD_F

CFD CODE USED

Numerical simulations has been performed with SHIPFLOW, a code that has been developed by FLOWTECH. SHIPFLOW includes three flow analysis modules: Free surface wave elevation can be computed with the potential flow solver (XPAN), thin boundary layer and transition can be evaluated with the boundary layer method (XBOUND) or the viscous flow resolved with the Reynolds Averaged Navier-Stokes (RANS) solver, (XCHAP).

The XCHAP code is a steady incompressible flow solver based on a finite volume method. The First order Roe scheme is used for the convective terms and a flux correction is added to obtain a higher order of accuracy. In the code three turbulence models are implemented, the kω-SST, kω-BSL models and the explicit algebraic stress model, EASM. No wall functions are used in the code and the model equations are integrated to the wall. The momentum, pressure and turbulence equations are solved in a coupled manner with the alternating direction implicit (ADI) method or Krylov solver.

Lifting Line Method

SHIPFLOW also includes a lifting line based propeller analysis module (LL). In this model, a finite-bladed propeller is first replaced with an infinite-bladed propeller. Then series of vortex systems, such as bound vortices, hub vortices and free (trailing) vortices, are distributed to represent the propeller. The slipstream contraction is not considered in this model because the pitch and the radius of each vortex line are assumed to be constant. Only the steady part of induced tangential and axial velocity is taken into account, although this method is mainly proved for lightly loaded propellers by Hough and Ordway (1965). The method used in the calculations of the induced velocities of propeller can be found in Dyne (1967). The determination of the non-dimensional blade circulation is made by incorporating a method based on Goldstein's Kappa theory (see Goldstein 1929). The viscous drag of the blade is calculated in an approximate way by an empirical formula for blade section drag. The principle of this method is briefly described by Zhang (1990) and Li (1994).

Modelling propeller/hull interaction by body force approach

The effect of the propeller is introduced in the RANS simulation as a body force for numerical modelling of propeller. By applying the body forces to discretized cells on the propeller disk, the flow is accelerated in the same way as suction of the flow by the propeller. The body force is calculated by propeller analysis code which is run iteratively with the RANS solver. The velocity computed by the RANS solver over the whole domain, subtracting the induced velocity estimated by the propeller analysis code, leads to an effective wake. This effective wake is used as the inflow to the propeller analysis code, which calculates axial and tangential body forces.

The interactive coupling between the RANS solver XCHAP and the lifting line model via body forces is completed with the following procedure at regular intervals, normally every 10 iteration in the RANS solver:

(i) Interpolate the current approximation of the velocity field to an embedded cylindrical grid concentric with the propeller.

(ii) Obtain the effective wake on the blade of the propeller by subtracting the propeller-induced velocities obtained in the previous iteration from the velocity field.

(iii) Run the propeller model in the effective wake and calculate the blade circulation, forces and torques.

(iv) Distribute the computed forces over the volume cells in the cylindrical grid.

(v) Interpolate the forces from the cylindrical grid to the computation grid and introduce them in the right-hand side of the N-S equations.

The fluid that passes through the propeller disk cells has thus acquired a body force and is accelerated so that the time averaged action of the propeller is simulated. The sum of the forces will give the fluid passing through the propeller disc a longitudinal and angular momentum consistent with the thrust and torque on the propeller.

The present method based on XCHAP/LL coupling has been validated through a number of test cases. Extensive comparative studies have been made by Han (2008).

Roughness Modelling

The roughness modelling has been implemented in the wall boundary condition for ω or k-ω and applying no slip boundary condition directly at the wall. Four alternatives are available in SHIPFLOW and they include the roughness model proposed by Hellsten, Knopp and Aupoix. All these models were tested by Orych (2019) in numerical uncertainty study for 2-D flat plate, KRISO containership KSC and tanker KVLCC2.

Following that study, the Aupoix-Colebook's model using a target non-dimensional near wall distance y+ of 0.5 is used for the present investigation.

Grid Topology

The overlapping grid technique with structured components was used to achieve high quality cells for ESD, propeller and rudder on the top of back ground grid for hull geometry. The overlapping grids consist of one back ground grid covered stern of the ship, refinement grid from back ground grid, a very fine component grids for the ESD, one propeller and one rudder.

A fine single-block structured H-O type grid (see

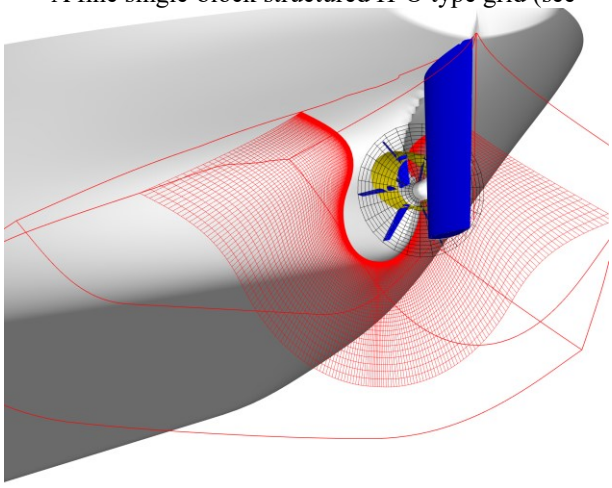

Figure 6) is used as a background grid which covered the entire ship hull (incl. propeller and rudder). The grid is generated using the grid generator module XGRID of the SHIPFLOW software. The XGRID is restricted to have constant x-planes which makes that the grid nodes does not match the stern contours. A stretching along the x-axis is used to refine the stern regions where the surface curvature is large and the hull shape needs to be represented more accurately. The grid covered both sides of the hull forms (asymmetric grid) and the total no. of cells used was 20.1M cells in model scale and 24.5M cells in full scale. The upstream boundary was at x/L_{REF} = -1.0 and the downstream boundary was at x/L_{REF} = 2.0 and the outer boundary was R/L_{REF} = 2.0 respectively.

The flow solver does not incorporate any wall functions and to resolve the boundary layer with satisfactory resolution the grids are highly stretched in the normal direction. The y+ value is kept around 0.5 for all computations.

The propeller is modelled by cylindrical grid using 12x32x31cells in the axial, radial and tangential direction. The propeller forces were transferred with an additional cylindrical grid with ~9000 cells.

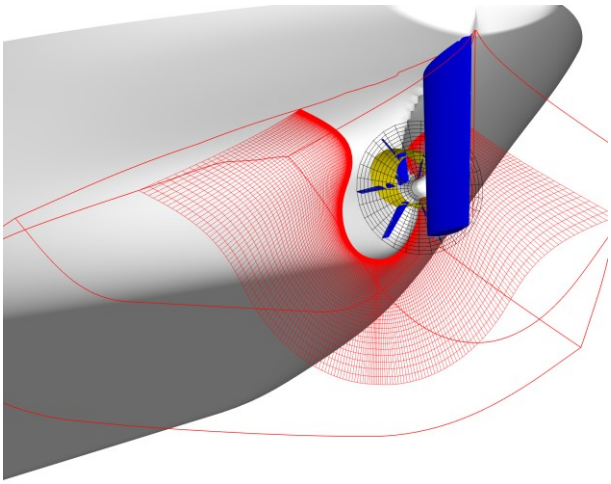

Figure 6: Hull, GK duct, propeller configuration – perspective view, refinement and the propeller inflow mesh visible.

SCALE EFFECTS ON ESD DESIGN

The scale effects of several different ESDs on energy saving mechanism have already reported in the previous papers (Kim et al., 2011, 2012 and 2014), and therefore only the most important findings will be discussed here.

Figure 7-**Figure 8** show the relative differences in percentages in the reduction of EHP and DHP based on SHIPFLOW computations for all four ESDs at model and full scale. In these figures, 0% indicates no difference while positive or negative sign indicate an increase or decrease of EHP and DHP relative to bare hull respectively. A clear contrast can be seen from **Figure 7** in the reduction of EHP between model and full scale. Small but clear reduction of EHP in model scale can be obtained by duct

type of ESDs, while this favorable effects of duct on EHP reduction is very Reynolds number dependent as can be seen: 1.5~1.8% increase for GKD_M and GKD_F in full scale. On the other hand, the PSS increases the EHP by 0.5% in model scale and 2.8% in full scale. Obviously, an increase in EHP when fitting an ESD is an unfavorable effect and this should be overcome by the improvement of propulsion efficiency. It should be also seen from **Figure 8** that the relative differences for DHP reduction between model and full scale are varying depending on ESDs. The duct is not actually working as an energy saver in full scale although the duct is quite effective in reducing the DHP by 3.6% in model scale. GKD_F shows largest energy saving (2.8%), as optimized for full scale performance, and the PSS in between in DHP reduction in full scale.

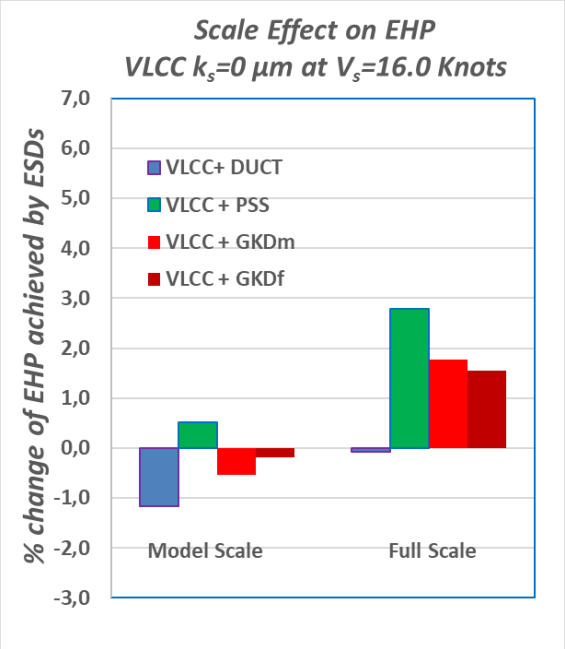

Figure 7: EHP reduction predicted for ESDs in model and full scale for VLCC at design condition (V_s=16.0 Knots, T_d=21.0m).

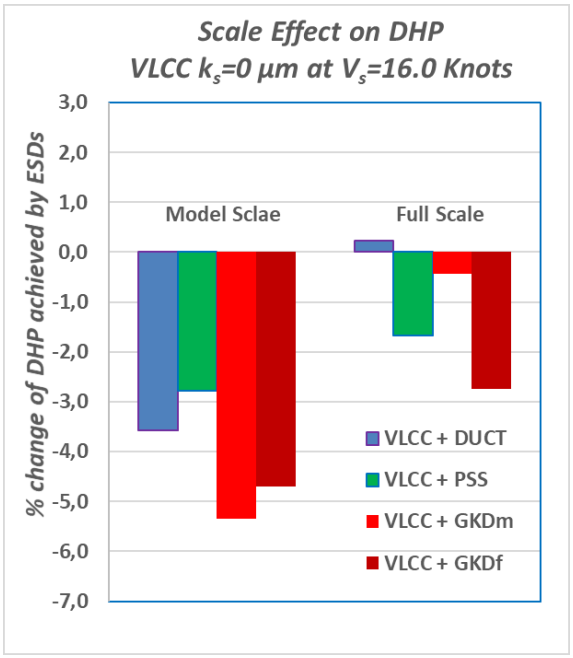

Figure 8: DHP reduction predicted for ESDs in model and full scale for VLCC at design condition (V_s=16.0 Knots, T_d=21.0m).

In order to validate whether GKD_M and GKD_F are doing what they should do as a real energy saver, confirmation tests have been performed (see **Figure 9**-**Figure 10**). Test methods and calculation principles for the resistance and self-propulsion tests were made according to ITTC 78 method and full scale performance prediction of the test results are made based on the modified wake scaling for pre-swirl stators suggested in the Specialist Committee on Unconventional Propulsors, 21st ITTC, 1999.

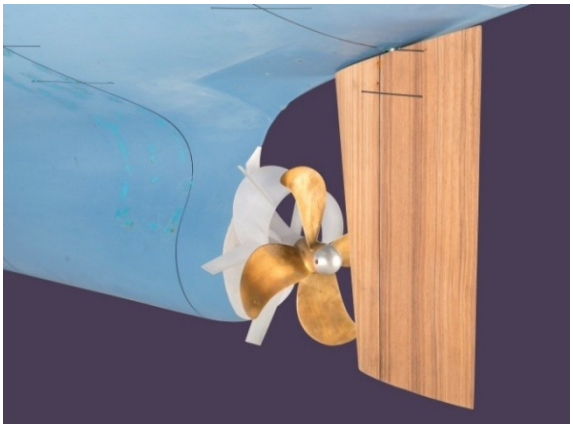

Figure 9: GKD_M mounted on a ship model for towing tank testing.

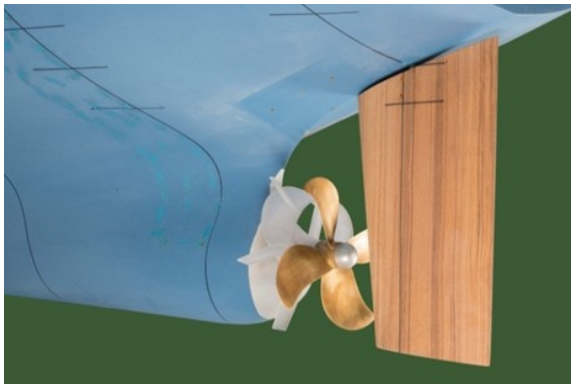

Figure 10: GKD_F mounted on a ship model for towing tank testing.

Comparison of power reduction by GKD_M and GKD_F is made in **Figure 11**-**Figure 12**. It can be seen that the savings predicted from towing tank tests are quite different from SHIPFLOW prediction. The figures illustrate very good correlation between SHIPFLOW simulation and model test results in model scale, while quite opposite results are obtained in full scale. The computation indicates that GKD_M is less effective in reducing the power as compared to GKD_F in full scale, which is in contradiction to the model test results.

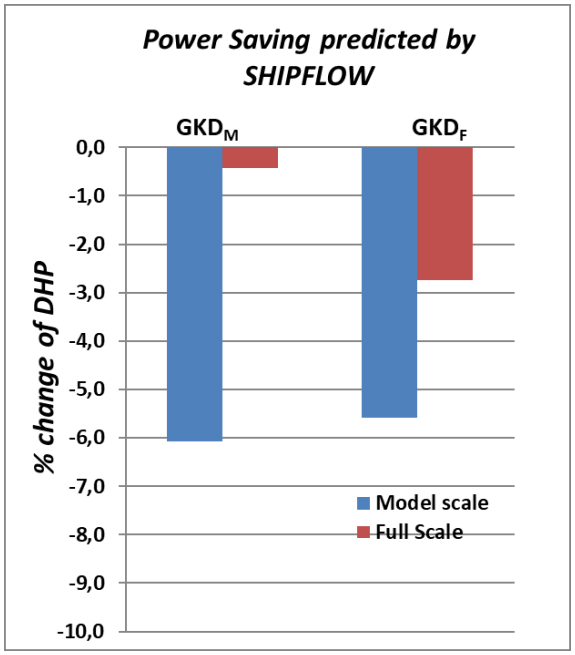

Figure 11: Power reduction estimated by SHIPFLOW for GKD_M and GKD_F.

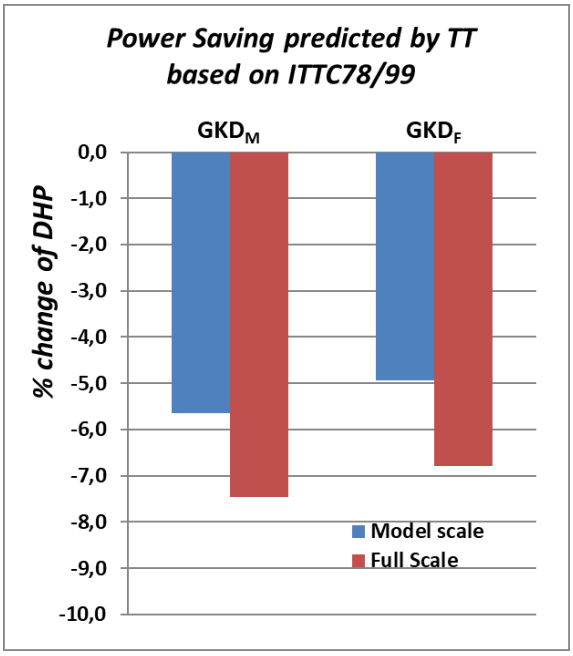

Figure 12: Power reduction estimated by model tests for GKD_M and GKD_F.

It is difficult to reliably predict full scale performance of this type of device from model tests at equivalent Froude number speed in the towing tank. Therefore, it is highly recommended to perform full scale CFD simulation to understand better how the energy saving mechanism works in full scale.

Understanding why the savings between model and full scale are varying dependent on type of ESDs is important in avoiding misinterpretation and over optimistic predictions. It has been claimed by the original developer, Scneekluth (1986) that the overall propulsive efficiency can be improved by the reduction of resistance, improvement of inflow uniformity and thrust generation by the duct. The physical interpretation of energy saving mechanism of duct in model and full scale has been made first by Kim et al (2012 and 2014) and later by Visonneau et al (2016). It turned out to be that the energy saving mechanism explained may be working but less efficiently in full scale. The separation in stern which occurs for the model may not occur, or may occur over a small region in full scale. The inflow characteristics to the propeller in full scale is more uniform. At full scale, hence a duct is less effective for energy saving.

Figure 13 presents total propulsion efficiency in full scale for different ESDs in comparison with the bare hull. It can be seen that there are practically no improvement by the duct, highest efficiency by the PSS and GKD_F and somewhere in between by GKD_M. The increase in propulsion efficiency can be explained by the increase of angle of tack of inflow to the propeller.

Figure 14-**Figure 15** shows mean angle of attack on propeller with different ESDs in model and full scale.

The duct does not improve the angle of attack as compared to the bare hull in both scales. There are large increases of angle of attack on propeller not only in model scale but also in full scale with the PSS compared to the bare hull. By increasing the angle of attack to the propeller, it can deliver the same thrust at a smaller rate of revolution. This directly resulted in the reduction of DHP as presented in **Figure 8** showing that 2.8% reduction in model scale and 1.7% reduction in full scale as compared to the base hull. It is promising results confirming that hydrodynamic effects of PSS on the improvement of propulsion performance are working in full scale as well as in model scale, and also that a PSS is less sensitive to scale effects.

When comparing GK ducts, the smaller DHP reduction predicted by GKD_M in full scale (see **Figure 11**) can be explained due to the fact that small increase in angle of attack especially in outer radii r/R > 0.6 is not sufficient to overcome the relatively larger increase of EHP as can be seen **Figure 15**. This directly resulted in 0.5% DHP reduction as compared with 2.7% for GKD_F.

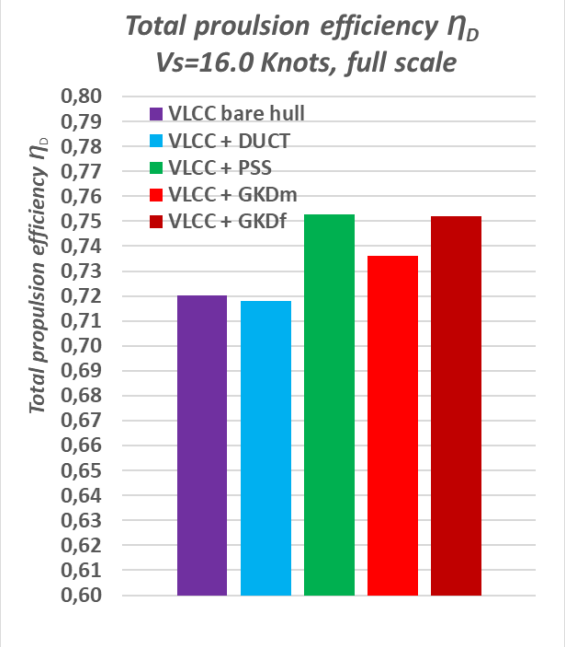

Figure 13: Total propulsion efficiency η_D predicted for ESDs

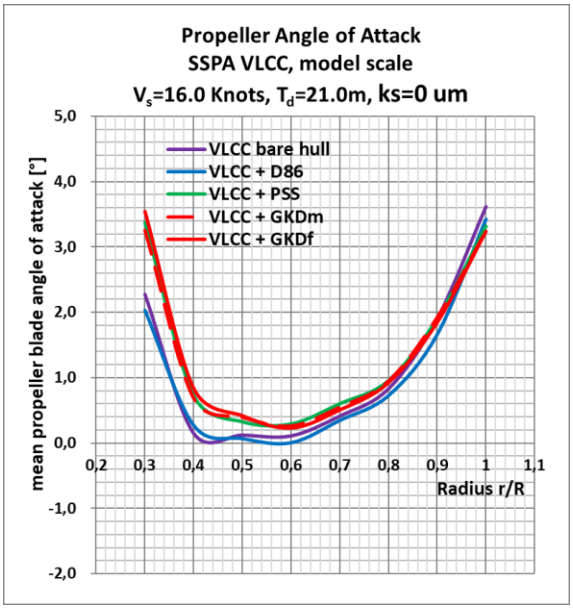

Figure 14: Propeller blade angle of attack predicted by CFD for different ESDs with smooth surface in model scale

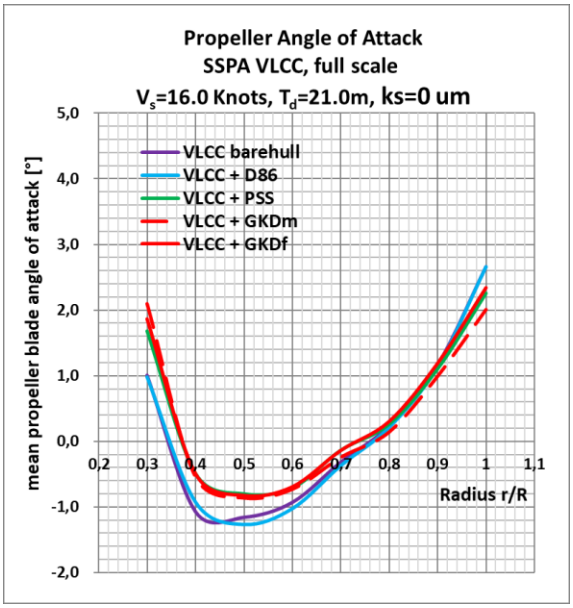

Figure 15: Propeller blade angle of attack predicted by CFD for different ESDs with smooth surface in full scale

ROUGHNESS EFFECT ON ESD DESIGN

After the scale effect exercise, the next step is to study how the roughness affects the flow around the hull and ship performance in both model and full scale. Roughness on vessels are normally quantified with Average Hull Roughness (*AHR*) which is usually measured by a roughness analyzer. However, *AHR* is not the same as

the equivalent sand roughness k_s used as a roughness input for CFD simulation and there is no universally applicable conversion relation between *AHR* and k_s. This is in itself another important area for future research.

Typical values of *AHR* for ship in service are given in **Table 1**. According to the virtual simulation study performed in the previous research (Kim et al 2019) based on direct scaling of relation between added resistance and roughness obtained, the corresponding roughness height k_s is estimated and attainable operating speed at NCR power with 15% sea margin and 1% of loss in shaft power. SHIPFLOW simulations have been performed for the tanker case with sand roughness height, k_s, ranging from 0 to 750 μm.

Table 1: Typical roughness values in actual ship operation

Type	*AHR*[μm]	k_s[μm]
New build vessel, state of the art of ship yards	60~100	12~20
Most probable operating hull surface level	200~400	100~300
Extremely rough surface condition	400~500	400~650

Resistance coefficients C_F, C_{PV} and C_V, rough surface

The roughness effects on skin friction, pressure and viscous resistances in model and full scale are presented in the form of the increase in the ratio between smooth and rough surface as shown in **Figure 16**. As expected the skin friction resistance coefficient C_F increases quite significantly with the growth of k_s, and it can be seen that the viscous pressure resistance coefficient C_{PV} increases equally fast. Another observation is that the increase of resistance coefficients, as roughness grows, is much higher in full scale compared to model scale.

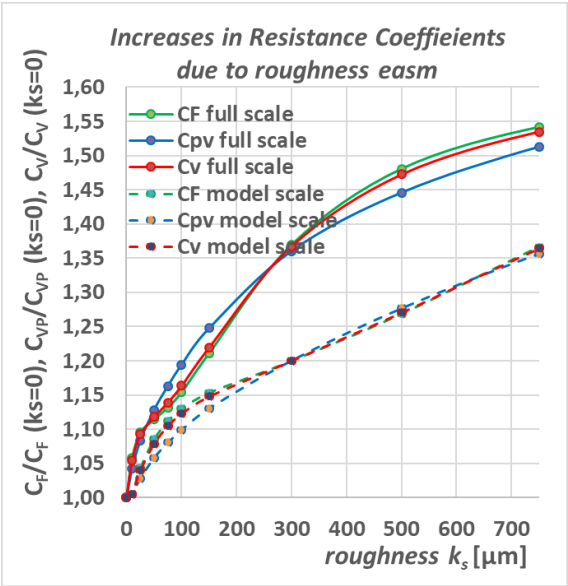

Figure 16: Increase of resistance coefficients C_F, C_P and C_V with the growth of k_s for tanker at design condition in model scale (dotted line) and full scale (solid line).

Model Test

Towing tank tests were carried out with two surface conditions applied to the ship model: smooth and rough surface (Werner, 2019). The smooth surface is the same surface condition of the ship model used for standard model testing at SSPA and is regarded as hydrodynamically smooth. The rough surface is a coating mixed with sand grains, which was applied to the ship model, see **Figure 17**. The roughness measured with a BMT roughness analyzer was *AHR* = 475μm for the ship model.

Flow quantities measured were resistance coefficients, propulsive factors and wakes from towing tank tests. The increase of total resistance R, propeller thrust T, torque Q and rpm estimated by SHIPFLOW in model scale with the growth of k_s is presented in **Figure 18** and compared with model test results.

Figure 17: Anti slip paint applied for VLCC model.

Correlation between k_s and *AHR*

Comparing resistance directly for the towed model (CFD simulations includes all major resistance components including wave resistance), the corresponding k_s can be found as the crossing between the measured resistance, torque, thrust and rpm from model test and CFD. The crossing somewhat depends on which quantity is based on; k_s =650 µm for resistance R, k_s=660 µm for thrust T, k_s=630 µm for torque Q and k_s=630 µm for rpm. The authors will continue to work on this with the purpose of finding the relation valid for relevant ship surface.

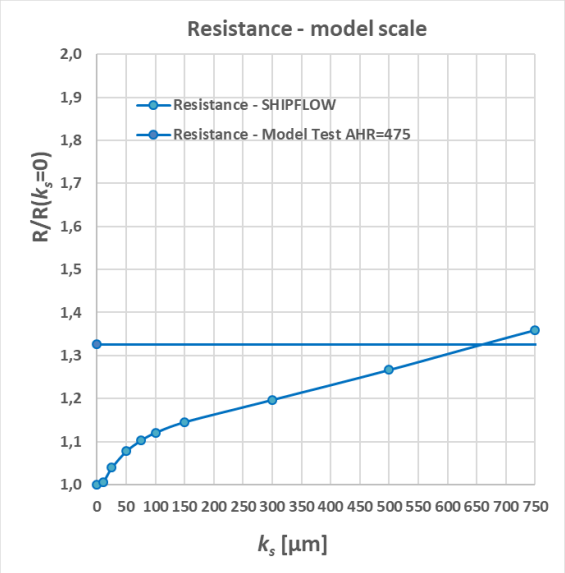

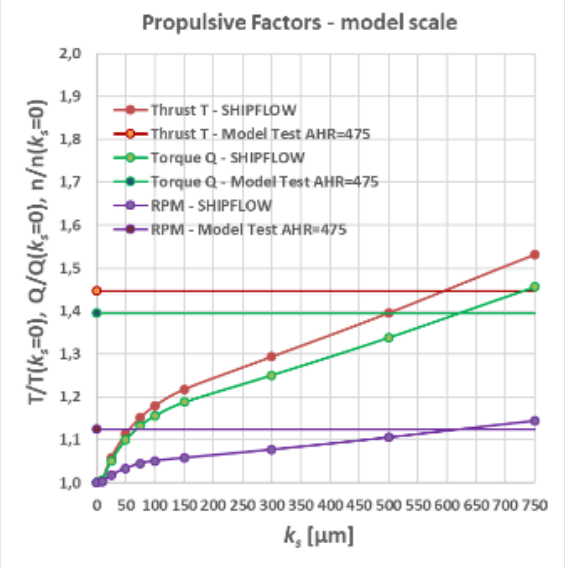

Figure 18: Increase of total resistance R and propulsion quantities (T, Q and rpm) estimated for a tanker by SHIPFLOW in model scale with the growth of equivalent sand grain roughness k_s and comparison with model test results with measured average hull roughness, *AHR*=475 µm.

Roughness Effect on Wake

The roughness also affects the flow in general and not only integrated resistance. **Figure 19** shows the measured wake for the tanker with anti-slip paint to the bottom and the predicted wake with k_s=650 µm to the top. The thickening of boundary layer can be clearly seen and the increase of the hook shape region by a shift of the position of vortex core center outward when comparing with the wake with smooth surface in **Figure 20**. This will result in the increase of mean wake. This trend can be seen from SHIPFLOW prediction as presented in the top in **Figure 20**. These significant differences (although at an extreme roughness) will severely affect propulsive efficiency and perhaps allow for operational design improvements.

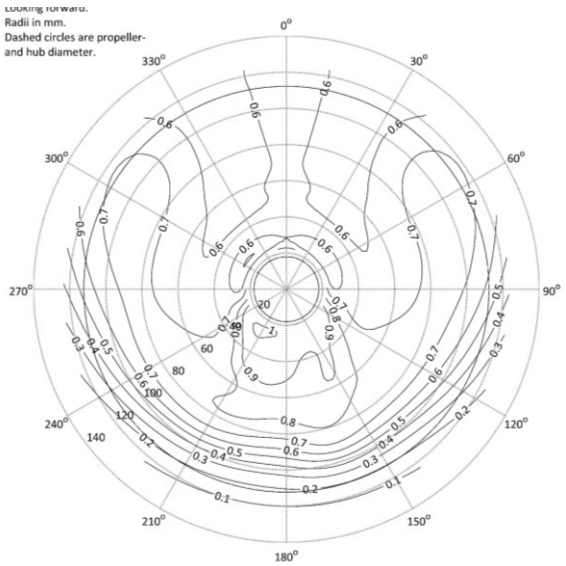

(a) SHIPFLOW simulation

(b) wake measurement

Figure 19: Comparison of measured nominal wake for model with rough paint *AHR*=475 µm and with CFD predicted wake for k_s=650 µm.

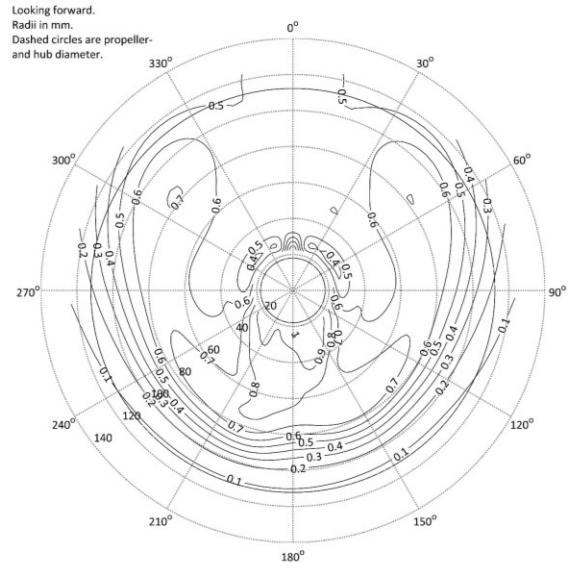

(a) SHIPFLOW simulation

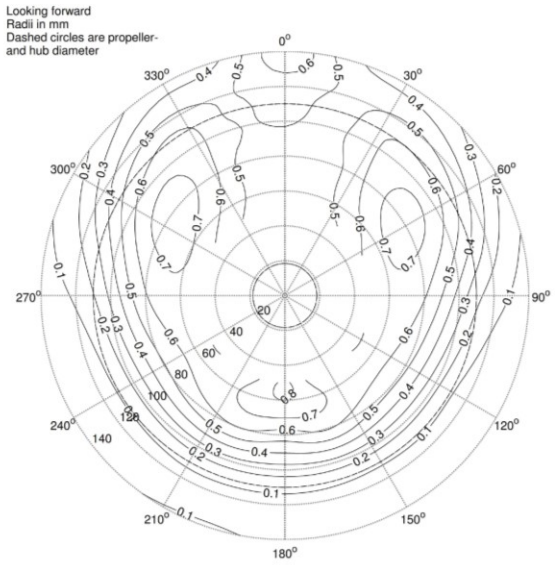

(b) Measurement

Figure 20: Comparison of total nominal wake of tanker with smooth surface condition k_s=0 µm at propeller plane in model scale.

Roughness Effect on Full Scale Ship Performance

The thicknening of boundary layer and strengthnening of bilge vortex with the growth of hull roughness height directly resulted in the increase of EHP as showin in **Figure 21**. Three areas of EHP increase can be observed, hydrodynamically smooth ($0 = k_s < 25$ µm), gradual increase up to k_s=100 µm, and linear increase thereafter. This difference in growth is best explained by the difference between intermediate and fully rough skin friction region.

Similar trends can be observed for propeller thrust (T), propeller torque (Q), propeller revolution (RPM) and deliverd power (DHP). This can be expected from the fact that the propeller should produce larger thrust and torque while rotating faster in order to overcome the resistance increase.

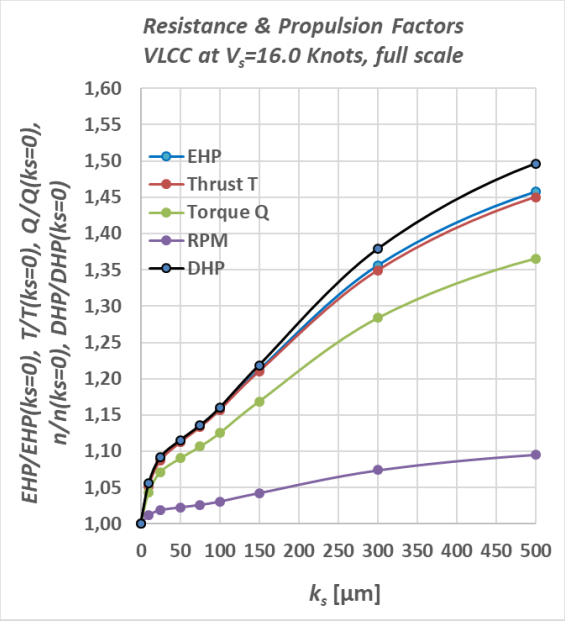

Figure 21: Increase of resistance/EHP, thrust T, torque Q, propeller revolution RPM and DHP with the growth of hull roughness height

However, this is not the speed (V_s=16.0 knots) and propeller rpm range in actual operation as the propeller should be running along the propeller characteristic power-rpm curves in the engine load diagram. The main engine and propeller can not be operated over the torque/rpm speed and overload limit in engine load diagram. The attainable operating ship speed at NCR power with 15% sea margin and 1% of loss in shaft power are given in **Figure 22**.

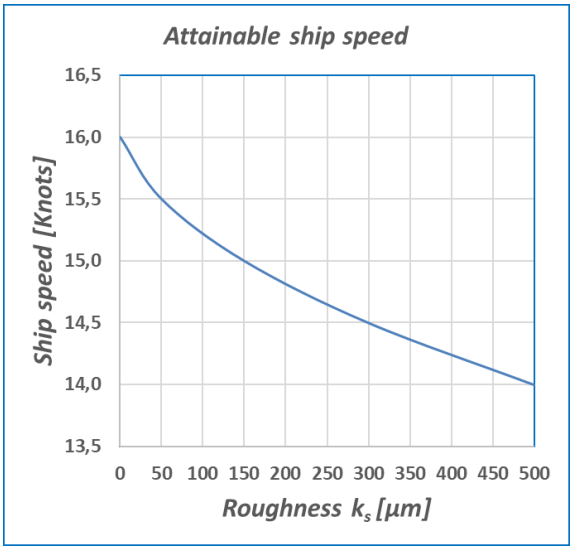

Figure 22: Attainable operating speed estimated at NCR for ship with corresponding roughness surface condition.

In addition to the scale effect discussed above, further investigations were performed to understand how the roughness affects the energy saving mechanism of the ESDs in model and full scale. For this purpose, SHIPFLOW simulations have been performed for four ESDs at attainable ship speeds with the corresponding sand roughness height k_s ranging from 0 to 500 µm.

Full Scale Wake for Bare Hull

How the full scale wake is affected by roughness is much less known or at least less considered in the design. **Figure 24Figure 25** illustrates a gradual change of wake characteristics at the propeller plane with hull roughness growth where the smooth case is shown in **Figure 23**. In **Figure 24-Figure 25** the strengthening of the bilge vortex with the increase of k_s can be clearly seen. The vortical flow becomes stronger and its center position moves more outward and upward with the increase of k_s comparing to model scale. This is a direct consequence of the thickening of the boundary layer especially in the region where the bilge vortex is formed.

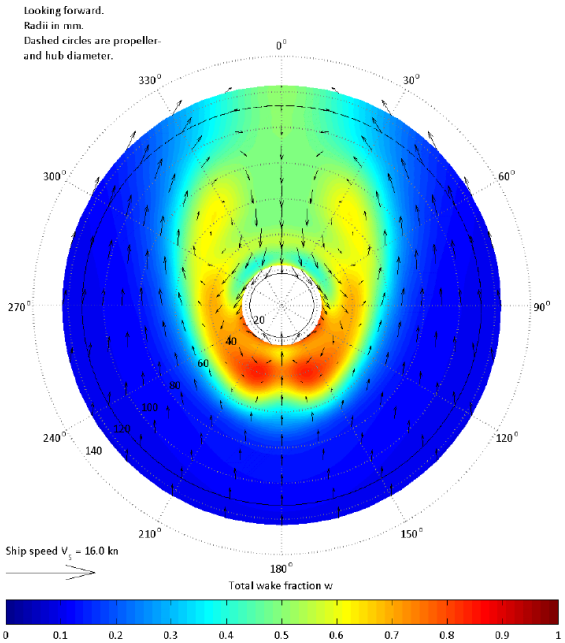

Figure 23: Full Scale, smooth surface k_s=0 µm and V_s=16.0 Knots

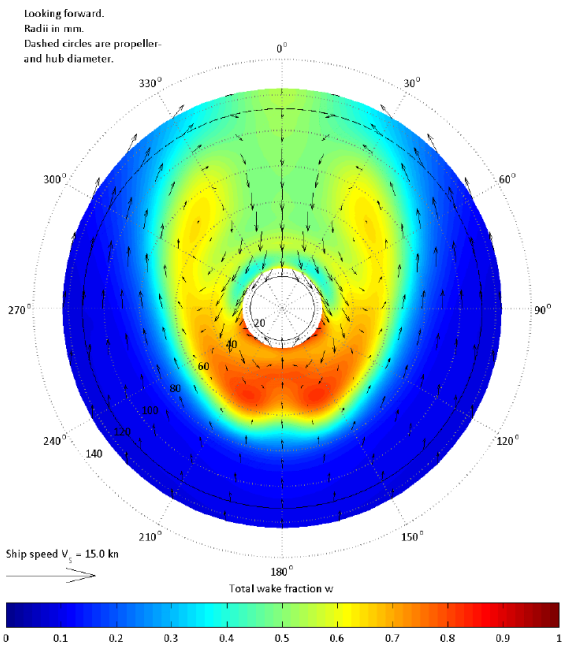

Figure 24: Full scale, k_s=150 µm and V_s=15.0 Knots

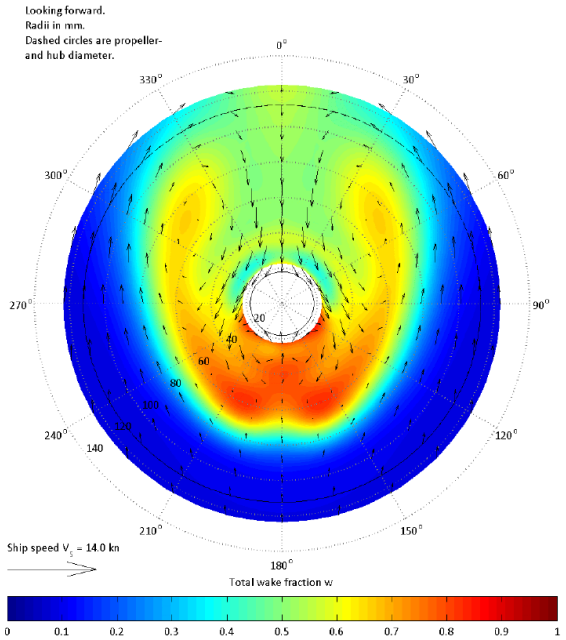

Figure 25: Full scale, k_s=500 µm and V_s=14.0 Knots

Roughness Effect on Energy Saving by ESD

In addition to the scale effect discussed earlier, further investigations were performed to understand how the roughness affects the energy saving mechanism of the ESDs in model and full scale. For this purpose, SHIPFLOW simulations have been performed for four ESDs at attainable ship speeds with the corresponding sand roughness height, k_s, ranging from 0 to 500 µm.

Figure 26-Figure 27 present the percentage difference of EHP, DHP and total propulsion efficiency η_D predicted for four ESDs relative to the bare hull at the same rougness surface condition. It is quite interesting to see that the roughness does not always cause negative effect (increase of resistance, EHP), but bring positive effect with energy saving (improvement of η_D and reduction of DHP) by ESDs. It is also interesting to see how the roughness affect the energy saving differently depending on type of ESD. Several interesting features can be observed:

Naturally, the EHP and DHP increase with the growth of rough height k_s. However, it is interesting to see the roughness effect of all ESDs from **Figure 26** that the relative increase of EHP of all to the bare hull decreases. Practically no relative decrease of EHP can be noted for the duct at smooth surface condition, but the reduction is increasing with the growth of hull roughness (1% at k_s=500 µm). Similar trends can be observed for the two GK ducts and the increase of EHP by GK ducts is in between duct and PSS, which seems to be quite reasonable.

Other interesting feature is small but clear trend to increase of relative improvement of total propulsion efficiency η_D predicted for all ESDs with the growth of hull roughness (see **Figure 27**). As a results, the reduction of DHP tend to increase with growth of hull roughness for ESDs (see **Figure 28**). In case of GKD_F, the expected power reduction can be 3.8% at at k_s=150 µm (most frequent operating condition), 4.3% at at k_s=300 µm and 4.8% at at k_s=500 µm. This is quite promising result highlighting the positive effect of roughness on power saving by ESDs.

Another finding is that the power reductions are varying dependent on type of ESD; a PSS is not as sensitive to roughness effects as a duct and SSPA generic ESDs.

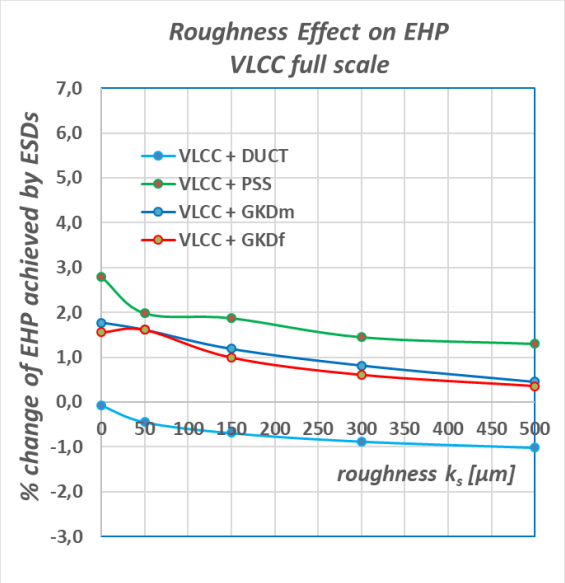

Figure 26: Percentage increase of EHP predicted for ESDs relative to the bare hull with the growth of hull roughness height.

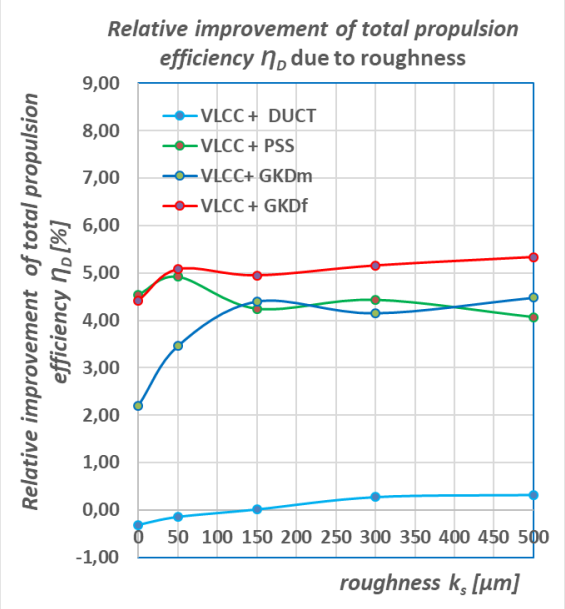

Figure 27: Percentage improvement of total propulsion efficiency η_D predicted for ESDs relative to the bare hull with the growth of hull roughness height.

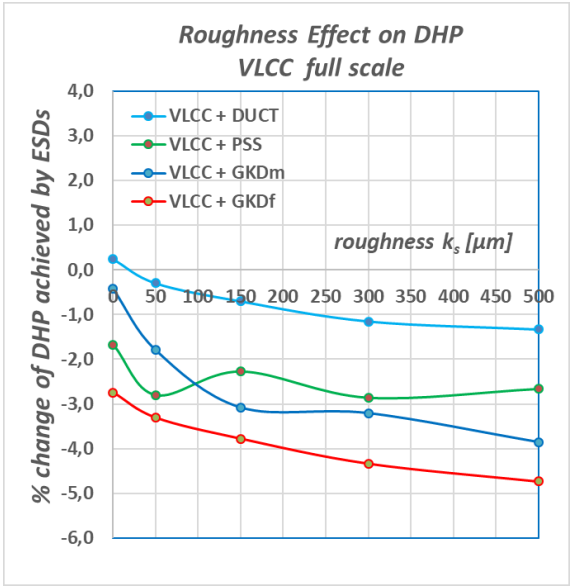

Figure 28: Percentage increase of DHP predicted for ESDs relative to the bare hull with the growth of hull roughness height.

The gain in propulsion efficiency and power reduction achieved can be explained by the increase of attack of inflow to the propeller. **Figure 29** and **Figure 30** show the predicted mean angle of attack on propeller behind ESDs at different roughness conditions. There are larger increases of angle of attack by PSS and GK ducts not only in model scale but also in full scale as compared to the bare hull case. By increasing the angle of attack to the propeller, it can deliver the same thrust at a smaller rate of revolution. This results in higher propulsive efficiency. The duct does not increase the angle of attack and thus result in relatively small improvement of total propulsion efficiency η_D.

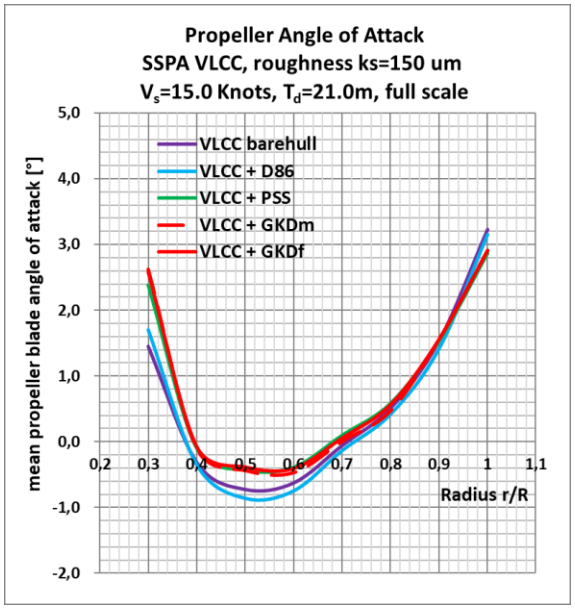

Figure 29: Roughness effect on angle of attack predicted by CFD between ESDs for VLCC with rough surface k_s=150 μm in full scale

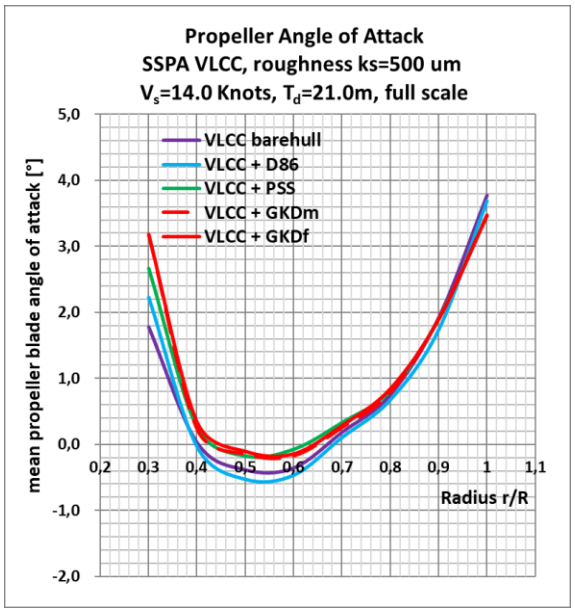

Figure 30: Roughness effect on angle of attack predicted by CFD between ESDs for VLCC with rough surface k_s=500 μm in full scale

Figure 31 shows how roughness and scale effect counter act on the energy saving for VLCC with GKD_F as compared with the bare hull. The DHP reduction predicted in full scale is about half in model scale for VLCC in smooth condition, but the decrease of power saving due to scale effect can be recovered during the operation of ship; ¼ of the scale effect when roughness growth to k_s=150 μm and about ½ at k_s=500 μm.

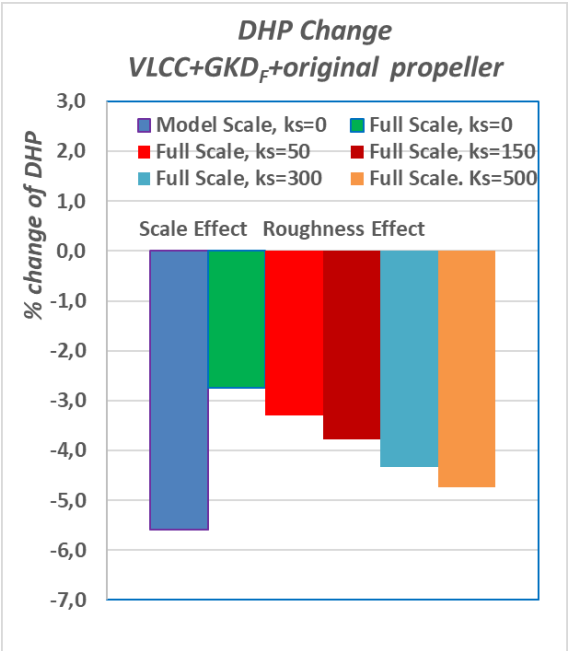

Figure 31: Change of DHP predicted for VLCC + GKD_F + original propeller due to scale and roughness effect.

REFINEMENT OF PROPELLER/ESD DESIGN FOR FULL SCALE ROUGH HULL CONDITION

In order to illustrate how the roughness effect can be taken into account in the design of ESD and propeller, an additional refinement study has been performed starting from GKD_F, the best optimized ESD for full scale performance. The main governing dimensioning and positioning design parameters are already investigated, a fine tuning of the design has been made for the wake at most probable operating hull roughness range 150~300μm. The design optimized for roughness effect was obtained from experienced based blending of duct geometry from GKD_M and stator geometry from GKD_F and was selected the final design, GKD_R, see **Figure 32**.

The predicted wake for GKD_R is presented in **Figure 33-Figure 34**. Comparing with the wake for smooth hull surface condition in **Figure 33**, the change in wake flow characteristics in rough hull surface condition (see **Figure 34**) is fairly favorable in view of pre-swirl flow generated in port side and less separation in starboard side.

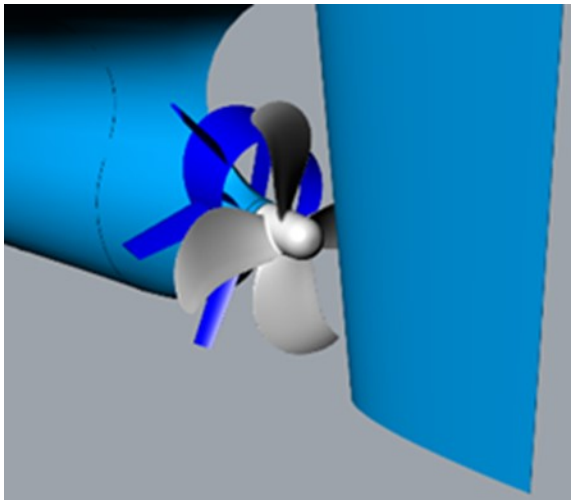

Figure 32: SSPA generic ESD, $GKD_{R,}$ which is refined for rough hull wake from GKD_F.

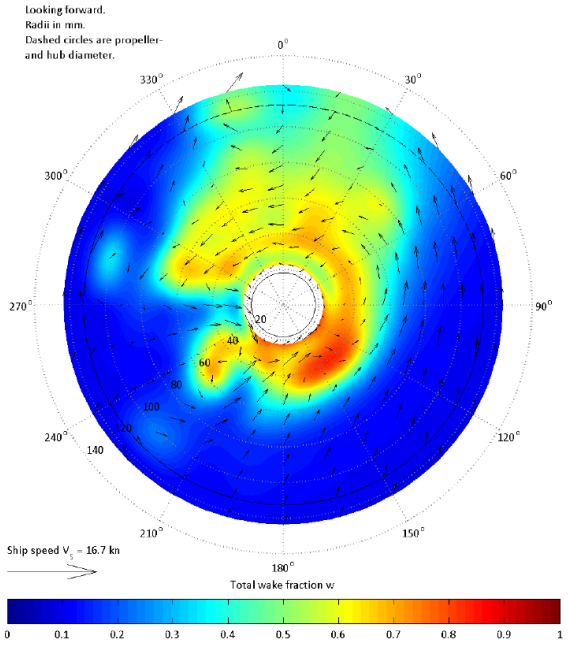

(a) GKD_F

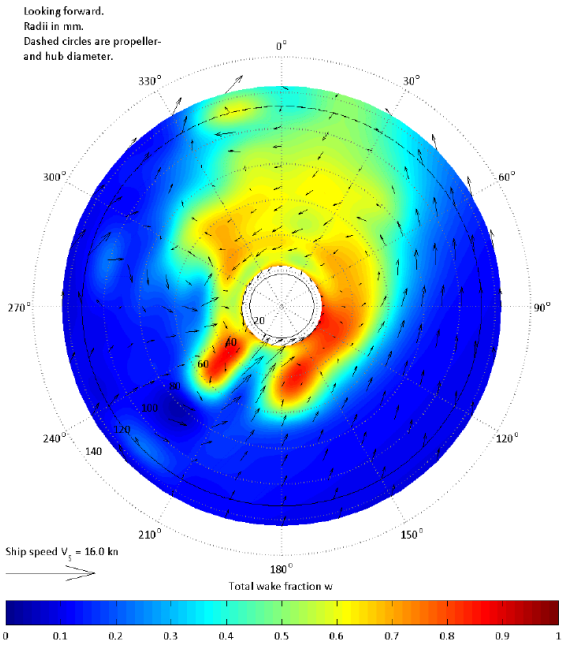

(b) GKD_R

Figure 33: Total wake and transverse velocities for VLCC with smooth surface k_s=0 μm and V_s=16.0 Knots at propeller plane.

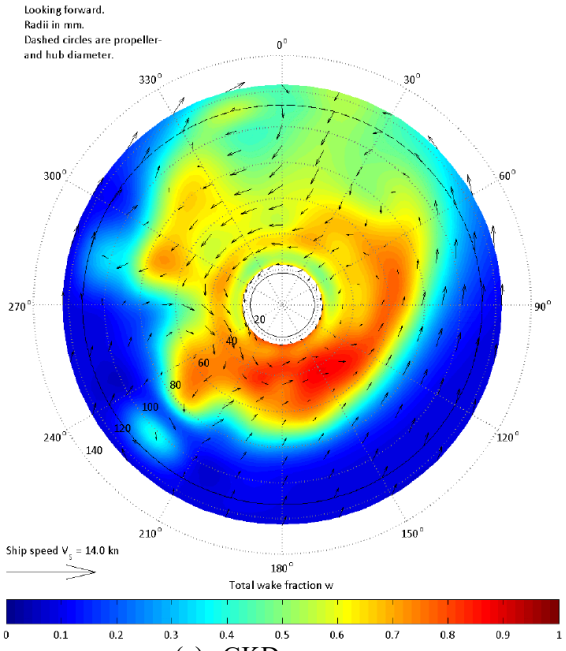

(a) GKD_F

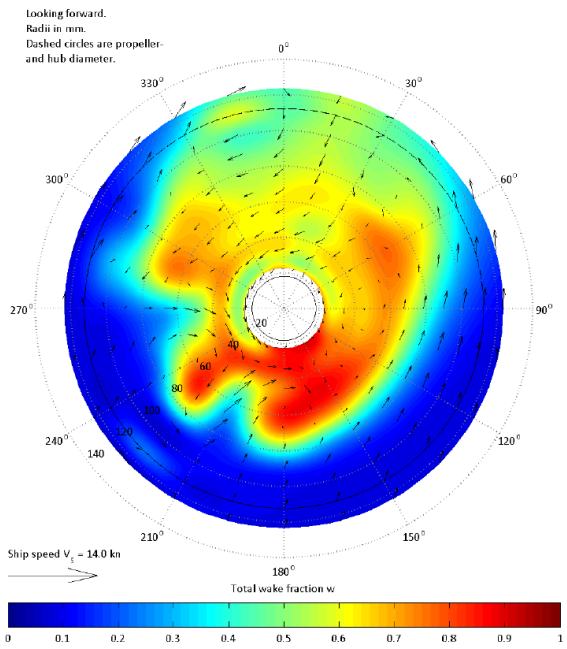

(b) GKD_R

Figure 34: Total wake and transverse velocities for VLCC with rough surface k_s=500 μm and V_s=14.0 Knots at propeller plane.

On the other hand, a relatively strong flow separation is visible in both smooth and rough surface conditions especially behind the inner part of the portside blade of GKD_R. This again resulted in relatively large increase in EHP as can be seen in **Figure 35**.

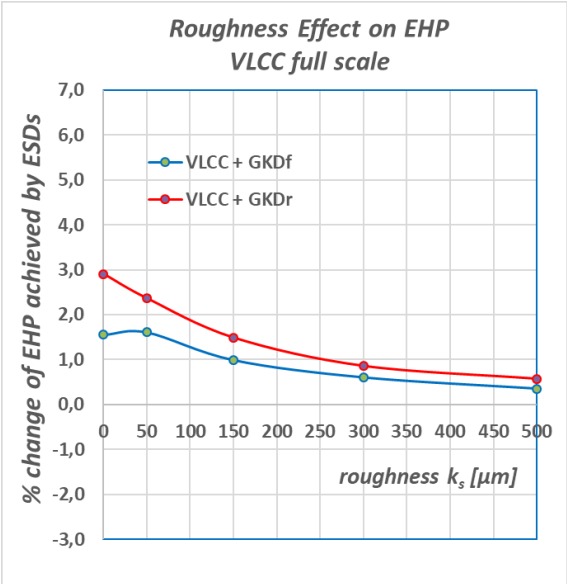

Figure 35: Percentage increase of EHP predicted for ESDs relative to the bare hull with the growth of hull roughness height.

Another illustration is presented is tuning of propeller design. The major change made is mainly the pitch and camber loading distribution for better hull-ESD-propeller interaction. The other dimensional design parameters (chord length, thickness and blade area ratio), no of blades and propeller diameter have been kept unchanged from the original propeller. The pitch and camber loading distribution is compared in **Figure 36-Figure 37**.

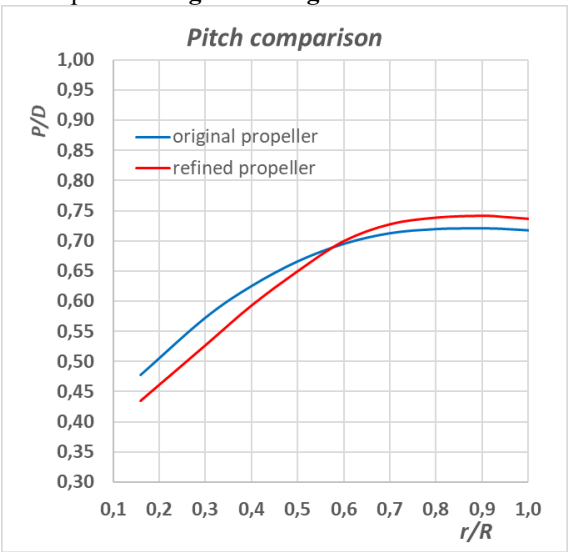

Figure 36: The design change made in pitch distribution for the refined propeller from the original propeller.

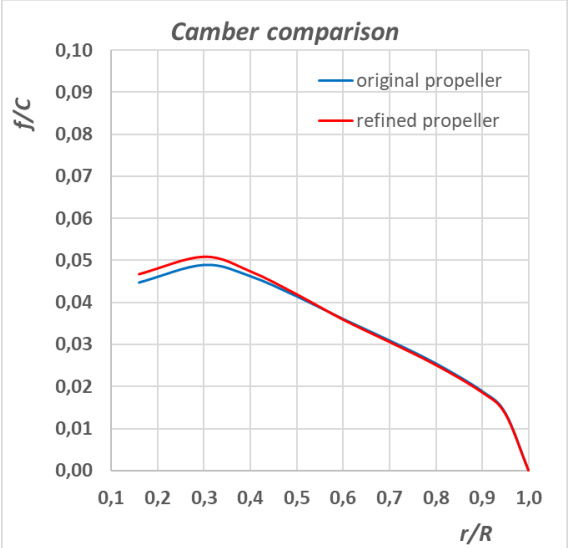

Figure 37: The design change made in camber distribution for the refined propeller from the original propeller.

The power reduction achieved from the design refinement made for GKD_R is compared with GKD_M and GKD_F in **Figure 38**. As expected from the fact that the refinement was made for full scale rough hull wake, the GKD_R is working most effectively with the growth of hull roughness height. The

DHP reduction predicted for GKD_R is 4.9% at k_s=300 µm and 5.6% at k_s=500 µm, which is 0.5% and 0.8% better than GKD_F. Further additional improvement by 0.2% can be achieved by the propeller refinement. And again total DHP reduction by GKD_R is 5.1% at k_s=300 µm and 5.8% at k_s=500 µm.

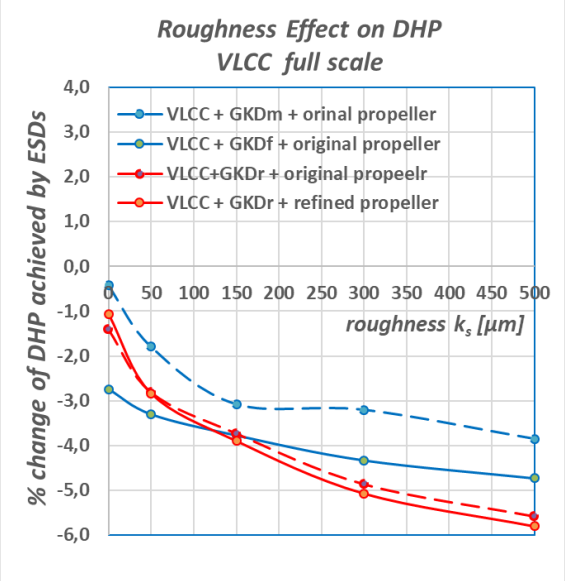

Figure 38: Power reduction compared for GKD and propeller at different hull roughness condition.

It can be seen that the higher power reduction by refinement of GKD_R and propeller can be explained by the further increase of propeller angle of attack as shown in **Figure 39Figure 40Figure 41**.

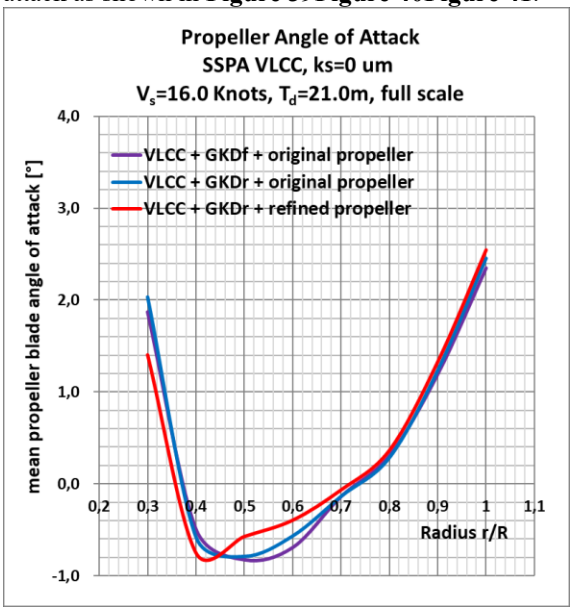

Figure 39: Change of mean propeller blade angle of attack by refined GKD_R and propeller, smooth surface at k_s=0 µm and V_s=16.0 Knots.

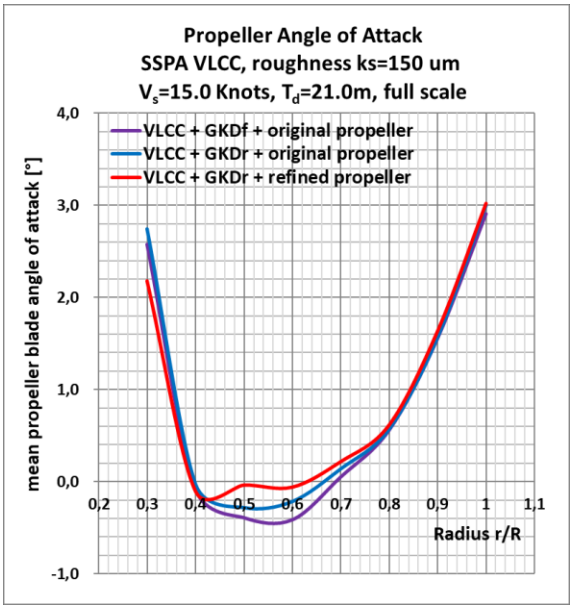

Figure 40: Change of mean propeller blade angle of attack by refined GKD_R and propeller, rough surface at k_s=150 µm.

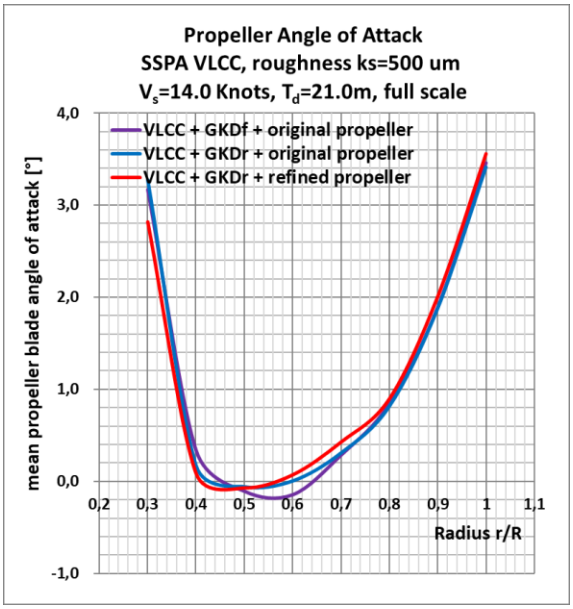

Figure 41: Change of mean propeller blade angle of attack by refined GKD_R and propeller, rough surface at k_s=500 µm and V_s=14.0 Knots.

Summarizing the results of the investigations made for scale and roughness effects, possible power savings predicted for all ESDs at different hull surface conditions are presented in **Figure 42**. It is very interesting results confirming that the most promising ESD for this particular ship is GK ducts and 3 to 5 % power saving can be achieved at most probable operational surface condition (100 µm < k_s < 300 µm). Although this does

not necessarily provide general conclusion as it may depend upon ship design and operational specifics, the present study could support shipbuilding and shipping industries by providing more accurate and reliable information about the expected return on investment. It should also be noted that the propeller and ESD design should be done based on optimum trade-off between the power reduction (favorable effect) and maximum allowable resistance increase/cavitation risk.

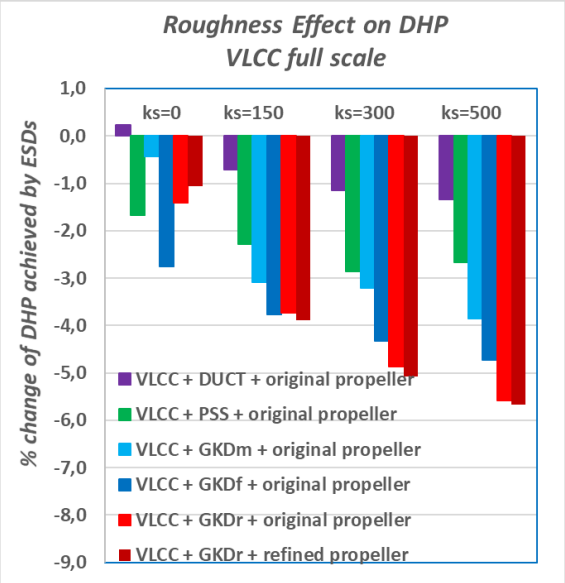

Figure 42: Possible DHP reduction predicted for different ESDs at varying rough surface conditions.

CONCLUSIONS

In the present paper, a design study of propeller and ESDs for a standard VLCC based on the proposed design methodology taking full consideration of both scale and roughness effects has been presented. Some interesting findings were obtained during the course of the work and the following conclusions can be drawn:

Scale Effect

- The energy saving of ESD is Reynolds number dependent: the ESDs investigated are quite effective in reducing the power in model scale, but less effective in full scale.

- The difference in savings between model and full scale are varying dependent on type of ESD; a PSS is less sensitive to scale effects than duct or combination of duct and PSS.

- As the ESDs operate around the stern of the ship where the change of flow characteristics by scale effects are most pronounced, the ESD design should be optimized for full scale.

Roughness Effect

- Surface roughness effects beyond the newly build condition are basically never considered in the design even though there is a possible risk of operating the propeller/ESD at higher loading condition. Other effects to take into account includes especially the effect of wake flow so that propeller and energy saving devices are designed for the correct flow field.
- Roughness on the full scale ship works in opposite direction as scale effects on the inflow to propeller and ESD. The DHP reduction predicted in full scale is about half in model scale for VLCC in new build condition, but the decrease of power saving due to scale effect can be recovered during the operation of ship; ¼ of the scale effect when roughness growth to k_s=150 µm and about ½ at k_s=500 µm.

Fundamental changes in ship design practice is suggested. The ship design should be optimized for actual operational condition taking into account operation issues especially hull surface condition. This approach in particular requires an early ship operator involvement in hull and propeller/ESD design.

FUTURE WORK

The relation between the equivalent sand roughness k_s used in CFD and the Average Hull Roughens *AHR* measured on real ships are still not fully understood. This is probably the largest source of uncertainty of all CFD studies of ship roughness and should be studied further. Moreover, the CFD models for roughness effects are derived based on flat plates. More research is needed on how the models perform for curved surfaces with adverse pressure gradients.

ACKNOWLEDGEMENT

This study was financially supported by TRAFIKVERKET, Sweden. The authors would like to express their sincere gratitude to TRAFIKVERKET for financial support and the productive cooperation.

REFERENCES

Kim Keunjae and Bathfield Nicolas (2011) “Refinement and Validation Study of CHAPMAN for Self-propulsion Test Simulation for Several Ship Type”, HHS 200, SSPA project report no RE40115569-01-00-A.

Kim Keunjae and Li Daqing (2012) “Validation Study of CHAPMAN for Self-propulsion Test Simulation for Energy Saving Devices”, HHS 205 SSPA project report no RE40115884-01-00-A.

Kim Keunjae, Bathfield Nicolas and Werner Sofia (2012): “Full Scale Self-propulsion Simulations for Energy Saving Devices”, HHS209, SSPA project report no. RE40116076-01-00-A.

Kim Keunjae, Leer-Andersen Michael, Werner Sofia, Orych Michal and Choi Youngbok (2012) “Hydrodynamic Optimization of Pre-swirl Stator by CFD and Model Testing”, Proceeding of the 29th Symposium on Naval Hydrodynamics, Gothenburg, Sweden, 26-31 August 2012.

Kim Keunjae, Leer-Andersen Michael and Orych Michal (2014): “Hydrodynamic Optimization of Energy Saving Devices in Full Scale”, Proceeding of 30th Symposium on Naval Hydrodynamics, Hobart, Tasmania, Australia.

Visonneau M, Deng G. B., Guilmineau E., Queutey P. and Wackers J. (2016) “Local and Global Assessment of the Flow around the Japan Bulk Carrier with and with out Energy Saving Devices at Model and Full Scale”, Proceeding of the 31th Symposium on Naval Hydrodynamics, Monterey, California.

Guiard Thomas, Leonard Steven and Mewis Friedrich (2013) “The Becker Mewis Duct® – Challenges in Full-Scale Design and new Developments for Fast Ships”, Third International Symposium on Marine Propulsors smp’13, Launceston, Tasmania, Australia.

Eca L., Hoekstra M. and Raven H. C. (2010) “Quantifying Roughness Effects by Ship Viscous Flow Calculations”, Proceeding of the 28th Symposium on Naval Hydrodynamics, Pasadena, California, USA.

Hough. G. R and Ordway. D. E.(1965) “The generalized actuator disk”, Development in Theoretical and Applied Mathematics. Vol II. 1965.

Dyne G (1967) “A method for the design of ducted propellers in a uniform flow”. Report No. 62, SSPA publications, Gothenburg, Sweden.

Goldstein. S. (1929): “On the vortex theory of screw propellers”. Proc. Roy. Soc. London. Series A 123.

Zhang D H (1990) “Numerical computation of ship stern/propeller flow”. Ph D thesis. Department of Naval Architecture and Ocean Engineering. Chalmers University of Technology.

Li. D-Q (1994) “Investigation on propeller-rudder interaction by numerical methods”, PhD thesis Department of Naval Architecture and Ocean Engineering. Division of Hydrodynamics. Chalmers University of Technology. Gothenburg. Sweden.

Han. K J (2008) “Numerical optimization of hull/propeller/rudder configurations”, PhD thesis, Department of Naval Architecture and Ocean Engineering, Division of Hydrodynamics, Chalmers University of Technology, Gothenburg, Sweden.

Orych Michal (2019): “Roughness Modeling in SHIPFLOW”, FLOWTECH Report No. 2019001.

Schneekluth, H. (1986) “Wake Equalizing Duct”, The Naval Architect, April, 1986 / A pamphlet from Schneekluth Hydrodynamik, Entwicklungs- und Vertriebsges. MBH.

Kim Keunjae, Leer-Andersen Michael and Werner Sofia (2019) “Roughness Effects on Ship Design and Operation”, Proceeding of the 14th International Symposium on Practical Design of Ships and Other Floating Structures”, Yokohama, Japan.

Werner Sofia (2018): “Model Test Report for SSPA standard VLCC”, SSPA project no. 40188895-00-01A.